



3 1176 00168 0892

NASA TM-81656

NASA-TM-81656 19810012549

NASA Technical Memorandum 81656

Exhaust Emission Survey of An F100 Afterburning Turbofan Engine at Simulated Altitude Flight Conditions

FOR REFERENCE

John E. Moss, Jr. and Richard R. Cullom
Lewis Research Center
Cleveland, Ohio

DO NOT BE TAKEN FROM THE BOOKS

JUN 15 1981

March 1981

NASA

Trade names or manufacturer's names are used in this report for identification only. This usage does not constitute an official endorsement, either expressed or implied, by the National Aeronautics and Space Administration.

EXHAUST EMISSION SURVEY OF AN F100 AFTERBURNING TURBOFAN ENGINE
AT SIMULATED ALTITUDE FLIGHT CONDITIONS

John E. Moss, Jr. and Richard R. Cullom

National Aeronautics and Space Administration
Lewis Research Center
Cleveland, Ohio 44135

SUMMARY

Emissions of carbon monoxide (CO), total oxides of nitrogen (NO_x), unburned hydrocarbons (HC), and carbon dioxide (CO₂) from an F100(1), afterburning, two-spool turbofan engine at simulated flight conditions are reported herein. Test conditions included simulated flight at Mach 0.8 for altitudes of 9.14 and 12.19 km (30 000 and 40 000 ft) and at Mach 1.4 at 12.19 km (40 000 ft). For each flight condition emission measurements were made for two or three power levels from intermediate power (nonafterburning) through maximum afterburning. These measurements were made by traversing a single-point gas-sample probe across the horizontal diameter of the exhaust nozzle.

The data showed that emissions vary with flight speed, altitude, power level, and radial position across the nozzle. Carbon monoxide emissions were low for intermediate power (nonafterburning) and partial afterburning, but regions of high CO were present downstream of the flame holder at maximum afterburning. Unburned hydrocarbon emissions were low for most of the simulated flight conditions.

The local NO_x concentrations and their variability with power level increased with increasing flight Mach number at constant altitude, and decreased with increasing altitude at constant Mach number. Emissions of CO₂ were proportional to local fuel-air ratio for all conditions.

INTRODUCTION

Testing of an F100 (1), afterburning, two-spool turbofan engine was conducted in an altitude facility to determine the oxides of nitrogen, unburned hydrocarbons, carbon monoxide, and carbon dioxide emissions at simulated flight conditions.

Emission tests were run at Mach 0.8 at altitudes of 9.14 and 12.19 km (30 000 and 40 000 ft) and at Mach 1.4 at 12.19 km (40 000 ft). For each simulated flight condition emission measurements were made for two or three power levels from intermediate power (nonafterburning) through maximum afterburning.

This investigation was conducted in the Propulsion Systems Laboratory at the NASA Lewis Research Center. Other exhaust emissions surveys previously reported on afterburning turbojet and turbofan engines can be found in references 1 to 6. The results of the present study augment the available literature on altitude emissions for afterburning turbofan engines.

N81-21078#

E-673

APPARATUS

Engine

The F100 (1), two-spool turbofan used in this investigation is shown in figure 1(a). The F100 is a 111 kN (25 000 lbf) thrust class; high overall pressure ratio (23:1); low bypass ratio (0.71:1) engine. This engine has a mixed-flow afterburner with V-gutter, flame-holders, and fuel-spray rings. The exhaust nozzle is a convergent-divergent, variable area, balance-beam type. The divergent-nozzle flaps on the test engine are free-floating. A more complete description of the engine appears in reference 7. The engine instrumentation locations are shown in figure 1(b).

Installation

The engine was installed in the altitude test chamber in a conventional direct-connect mode (fig. 1(a)). Conditioned air, required to simulate the selected flight conditions, was provided by the facility. Also, the engine exhaust pressure level required to simulate flight conditions was maintained. Engine exhaust gases were captured by a water-cooled collector to prevent their recirculation in the test chamber. These tests were run using JP-4 fuel (MIL-T-56246).

Gas Sampling System

A single-point, traversing, water-cooled, gas-sample probe was used in this study. The probe and its traversing mechanism are shown mounted behind the engine in figure 2(a). The traversing mechanism was capable of translating the probe ± 60 cm horizontally and ± 20 cm vertically from the engine centerline. A photograph and a schematic of the sensor area of the probe are shown in figures 2(b) and (c). The gas-sampling probe has an inside diameter of 0.72 cm (0.28 in.) and extended 1.9 cm (0.75 in.) forward of the probe support. The gas sample line was water-cooled for a distance of 8 cm (3.2 in.) from the probe tip. From this point the sample line inside diameter was 0.82 cm (0.32 in.) and was water-cooled an additional 30 cm (12 in.).

A total-pressure probe was mounted 2.5 cm (1.0 in.) above the sample probe, and three unshielded iridium/iridium-rhodium thermocouples were mounted 2.5 cm (1.0 in.) and 5.0 cm (2.0 in.) below and 5.0 cm (2.0 in.) above the gas-sample probe.

A schematic of the gas analysis system is shown in figure 3(a). Approximately 10 m of 0.95-cm stainless-steel line was used to transport the sample to the analyzers. To prevent condensation of water and to minimize adsorption-desorption effects of hydrocarbon compounds, the line was heated with steam at 428 K. Four heated metal bellows pumps were used to supply sufficient gas sample pressure (17 N/cm²) to operate the analytical instruments. The gas sample line residence time was less than 2 seconds for all test conditions.

Gas Analysis Instrumentation

Four commercially available instruments, along with associated peripheral equipment necessary for sample conditioning and instrument calibration are comprised in the exhaust-gas analysis system (fig. 3(b)).

The hydrocarbon (HC) content of the exhaust gas was measured on a wet basis using a flame ionization detector type instrument (Beckman Instruments model 402 hydrocarbon analyzer). Both carbon monoxide (CO) and carbon dioxide (CO₂) were measured dry, using analyzers of the nondispersive infrared (NDIR) type (Beckman Instruments model 315B). The concentration of the oxides of nitrogen (NO_x) was measured on a dry basis using a chemiluminescence analyzer (Thermo Electron Corporation Model 10A). This instrument includes a thermal converter to reduce NO₂ to NO. The exhaust gas constituents that were measured on a dry basis (CO, CO₂ and NO_x) were corrected for inlet air humidity and water vapor from combustion, and are reported herein on a wet basis.

The exhaust emission data measured by the analytical instruments were recorded and processed by an on-line facility computer. This computer was also used to control the traverse of the gas-sample probe and to determine the nozzle-exit diameter.

TEST CONDITIONS AND PROCEDURES

Exhaust-emission surveys were conducted at simulated altitude conditions of 9.14 and 12.19 km (30 000 and 40 000 ft) at Mach 0.8 and at 12.19 km (40 000 ft) at Mach 1.4. These test conditions were representative of typical subsonic and supersonic aircraft operating points. This choice of conditions gives a variation in altitude at a constant subsonic Mach number and a variation in simulated Mach number at a constant altitude. The test points and nominal inlet conditions are presented in table I. Conditioned air was supplied to the plenum at the desired pressure and temperature. The test chamber was maintained at the pressure required for true simulation of the selected altitude condition. This pressure resulted in the nozzle being choked for all survey data presented.

TABLE I. - TEST CONDITIONS

Simulated Mach number	Simulated altitude		Metered fuel-air ratio	Engine inlet pressure		Combustor inlet temperature		Primary combustor pressure		Afterburner mixed inlet pressure		Afterburner mixed inlet temperature	
	m	ft		N/cm ²	psia	K	°R	N/cm ²	psia	N/cm ²	psia	K	°R
0.8	9 140	30 000	0.0124	4.57	6.62	752	1354	117	169	13.6	19.67	736	1325
	9 140	30 000	.0603	4.54	6.59	752	1354	115	167	13.7	19.92	744	1340
	12 190	40 000	.0125	2.83	4.10	728	1311	75	109	8.7	12.57	725	1305
			.0337	2.80	4.07	727	1309	75	109	8.6	12.46	726	1307
↓			.0620	2.81	4.08	729	1313	77	111	8.8	12.74	734	1322
1.4			.0111	5.95	8.63	795	1432	119	173	13.8	20.02	729	1313
1.4			.0307	5.91	8.57	793	1427	114	165	13.6	19.65	723	1302
1.4	↓	↓	.0549	5.95	8.63	793	1427	119	172	14.0	20.35	737	1327

Emissions surveys were made at two or three power settings at each simulated flight condition. Power levels included intermediate (maximum power, nonafterburning), partial afterburning (afterburning zones 1, 2, and 3) and maximum afterburning (all five zones of afterburning). Gas sampling surveys were made slightly downstream of the nozzle-exit plane. For the nominal maximum afterburning condition the nozzle was near wide open, and the axial distance from the nozzle lip downstream to the survey plane was 5.6 cm (2.2 in.). At the partial afterburning power level the nozzle area decreased from maximum, and the axial distance from the nozzle lip to the survey plane was 6.4 cm (2.5 in.). At intermediate power the nozzle was near its minimum area, and the distance from nozzle lip to survey plane was 8.8 cm (3.5 in.).

The exhaust-nozzle diameter was obtained using the survey rake in conjunction with two nozzle-mounted air jets. Aft-facing high-pressure air jets were mounted on two diametrically opposite divergent nozzle leaves coinciding with the horizontal survey diameter. Just before a gas-sample survey a continuous traverse was made, and the position of the air jets marking the nozzle-exit diameter were noted as pressure spikes sensed by the total-pressure probe of the survey rake.

Surveys were made across the horizontal diameter of the exhaust nozzle. Twenty-one data points were recorded for afterburning to delineate the steep gradients in the emission profile. This resulted in a nominal spacing of 4.8 cm (1.9 in.) for maximum afterburning and 4.3 cm (1.7 in.) for partial afterburning. A 21-data-point traverse required approximately 30 minutes to complete. Eleven data points were recorded for nonafterburning as the gradients in the emission profiles were less steep. The nominal data point spacing at intermediate power was 6.6 cm (2.6 in.).

RESULTS AND DISCUSSION

Profile Data

Selected exhaust profile data are shown in figures 4 to 11. A complete tabulation of the experimental data obtained in this investigation is included in appendix A. This appendix also contains the average data (mass weighted and area integrated). Concentrations of CO, CO₂, and NO_x are given as parts per million by volume (ppmv), and the HC concentrations are given as parts per million carbon by volume (ppmCv). The horizontal axes in the figures are the radial distances from the centerline nondimensionalized by the measured nozzle-exit radius R_g for each test. This radius varies with flight condition and engine power level.

Exhaust total temperature. - The total-temperature distribution across the nozzle at each power level is shown in figure 4. At intermediate power the temperature distribution is nearly uniform across the exhaust plane. For partial afterburning the temperature profile shows twin regions of high temperature. The low temperature in the center region indicates that there was very little combustion in the wake behind the center body. For maximum afterburning the temperature profile is nearly flat at high-temperature levels, indicating radially uniform combustion. The temperature profiles were not affected significantly by Mach number and altitudes.

Fuel-air ratio. - The local fuel-air ratio calculated from the gas-sample measurements (FAREMISS) using the relationship in reference 8 are shown in figure 5. The similarity of the fuel-air ratio and the temperature profiles and the increase in the average temperature with increasing power level is expected, since increasing the fuel-air ratio should increase the temperature for all fuel air-ratios less than stoichiometric.

Carbon monoxide. - The variations of the carbon monoxide (CO) emissions with power level for each flight condition are shown in figure 6. Carbon monoxide emissions were less than 500 ppmv at all radii for intermediate power (nonafterburning), and at radii less than a $0.5R_g$ in afterburning. Downstream of the ring flame holders, a slight increase in CO concentration is apparent at partial afterburning for Mach 0.8 at 12.19 km, but at maximum afterburning, twin regions of high CO concentrations in the wakes of the ring flame holder were present with peak CO concentrations in excess of 11 000 ppmv for all flight conditions. Since the local fuel-air ratios were approaching stoichiometric in these regions, these high CO levels represent

an approach to equilibrium CO, rather than combustion inefficiency. Examination of these profiles shows that concentrations were highest at Mach 0.8 at 9.14 km and lowest at Mach 1.4 at 12.19 km.

Hydrocarbons. - Measured hydrocarbon emissions (fig. 7) were zero at all radii for nonafterburning conditions and at all radii less than 0.6Rg for maximum afterburning. For afterburning, regions of HC emissions representing inefficient combustion are present out board of the CO peaks. At radii greater than 0.6Rg for afterburning power levels, HC concentrations varied widely, with peak values in excess of 4000 ppmCv for all flight conditions.

Oxides of nitrogen. - The variations of the oxides of nitrogen (NO_x) emissions (concentrations) with power level at each flight condition are shown in figure 8. For Mach 0.8 at 9.14 km the peak NO_x emissions were higher at maximum afterburning than at intermediate power. For Mach 0.8 at 12.19 km, the peak NO_x emissions were about the same for all power levels, with local maxima near $R/R_g = 0.6$ for afterburning and in the center region at intermediate power. For Mach 1.4 at 12.19 km, the NO_x emissions decreased from intermediate power to partial afterburning at almost all radial locations. For this flight condition the maximum NO_x concentrations were observed at maximum afterburning. The same data as in figure 8 are shown grouped by power level in figure 9. For all power levels NO_x concentrations are consistently highest at the Mach 1.4 at 12.19-km condition, and lowest at the Mach 0.8 at 12.19 km condition, as might be expected since these are the conditions with, respectively, the highest and lowest combustor and afterburner inlet temperatures and pressures (see table I). Although the inlet conditions at the Mach 0.8 at 9.14 km test point are quite similar to those at Mach 1.4 at 12.19 km, note that the combustor-inlet temperature is slightly less at Mach 0.8 at 9.14 km and that peak NO_x concentrations at this condition are less than at Mach 1.4 at 12.19 km for both intermediate power and maximum afterburning (no comparison can be made at partial afterburning). Note in the maximum afterburning curves that there appears to be a deficiency of NO_x in regions of very high CO, which is consistent with the results in reference 6.

Carbon dioxide. - The variations of CO_2 emissions with flight conditions at each power level are shown in figure 10. The CO_2 emission profiles are similar, as expected, to the fuel-air ratio profiles (fig. 5) and show little variations with Mach number and altitude. The CO_2 distributions are radially uniform at intermediate power, but at partial afterburning the CO_2 profiles have twin regions of high emissions.

Exhaust total pressure. - For all flight conditions the measured exhaust total pressure P_{tg} at intermediate power was greater than the total pressure for afterburning conditions (fig. 11), as a result of pressure loss due to combustion in afterburning. All of the profiles show a low-pressure region at the centerline of the exhaust nozzle, in the wake of the engine centerbody.

Correlations with Local Fuel-Air Ratio

As discussed previously, the measured values of CO, HC, and CO_2 at each radial location (figs. 6, 7, and 10) were used to calculate emissions based local fuel-air ratios (FAREMISS; see fig. 5). Mass weighted and area integrated values are compared with the metered fuel-air ratios (FAABT) in figure 12.

Figures 13 to 16 show the emissions data plotted against the local fuel-air ratio for all flight conditions and power levels tested. Carbon mon-

oxide emissions (fig. 13) were low for local fuel-air ratios (FAREMISS) less than 0.047, but increased sharply for local fuel-air ratios greater than this value.

Carbon dioxide emissions increased linearly with increased values of local fuel-air ratios (fig. 14) except for deviations at high fuel-air ratios in regions of high CO₂.

Hydrocarbon emissions were essentially zero for all intermediate power conditions and showed considerable scatter in afterburning (fig. 15). No correlation between the HC emission and local fuel-air ratio (FAREMISS) was apparent.

The oxides of nitrogen emissions increased linearly with FAREMISS at intermediate power conditions (no afterburning), but variations with local fuel-air in afterburning were small (~ ±100 ppmv) for each flight condition (fig. 16).

The effects of flight speed and altitude (i.e., combustor and afterburner inlet temperature and pressure) on NO_x emissions are most apparent at intermediate and maximum afterburning power, with maximum NO_x observed at Mach 1.4 at 12.19 km and minimum values recorded at Mach 0.8 at 12.19 km (see table I). The concentrations of NO_x at Mach 0.8 at 9.14 km were less than at Mach 1.4 at 12.19 km, for both intermediate power and maximum afterburning as mentioned previously.

The combustion efficiencies calculated from gas sample data with and without afterburning are shown in table II. The local concentration data (CO, CO₂, HC, and NO_x) were mass weighted and area integrated to obtain average concentrations. These average concentrations were used to calculate combustion efficiencies. For the test conditions reported the efficiencies did not vary with changes in simulated flight conditions.

TABLE II. - COMBUSTION EFFICIENCY (WITH AND WITHOUT AFTERBURNING)

Simulated Mach number	Altitude		Combustion efficiency	Afterburner mixed inlet pressure		Power level
	km	ft		N/cm ²	psia	
0.8	9.14	30 000	99	13.6	19.67	Intermediate
↓	9.14	30 000	97	13.7	19.92	Maximum afterburning
	12.19	40 000	99	8.7	12.57	Intermediate
↓	↓	↓	98	8.6	12.46	Partial afterburning
			97	8.8	12.74	Maximum afterburning
1.4	↓	↓	99	13.8	20.02	Intermediate
1.4			98	13.6	19.65	Partial afterburning
1.4	↓	↓	98	14.0	20.35	Maximum afterburning

SUMMARY OF RESULTS

Gaseous emissions for an F100 (1), afterburning, two-spool turbofan engine were measured at simulated flight conditions. For each flight condition detailed concentration profile measurements were made for two or three engine power levels from intermediate (nonafterburning) through maximum afterburning. These measurements were made on the horizontal diameter at the engine exhaust-nozzle exit, using a single-point traversing sample

probe. The data showed the emissions vary with flight speed, altitude, power level, and radial position across the nozzle. The principle results of this investigation are as follows:

1. Carbon monoxide emissions were low for intermediate power (non-afterburning) but increased with afterburning primarily due to the appearance of high carbon monoxide regions downstream of the flame holder.

2. Oxides of nitrogen emission increased with increasing flight speed at constant altitude and decreased with increasing altitude at constant speed.

3. The variations of the oxides of nitrogen emissions with power level were different for the several flight conditions, but in all cases the maximum concentrations occurred at maximum afterburning.

4. Measured hydrocarbon emissions were zero at all nonafterburning conditions. In afterburning hydrocarbon concentrations were low in the center half of the nozzle, but varied widely in outboard regions.

5. Total temperature, local fuel-air ratio, and carbon dioxide distributions showed little variation with Mach number and altitude.

6. The exhaust temperature profiles are nearly uniform for maximum afterburning, which indicated uniform combustion.

APPENDIX - Experimental Data

The engine inlet conditions and the exhaust profile data for all flight conditions and power levels are given in tables III to V in this appendix.

REFERENCES

1. Diehl, Larry A.: Preliminary Investigation of Gaseous Emissions from Jet Engine Afterburners. NASA TM X-2323, 1971.
2. Palcza, J. Lawrence: Study of Altitude and Mach Number Effects on Exhaust Gas Emissions of an Afterburning Turbofan Engine. NAPTC-ATD-212, Naval Air Propulsion Test Center, 1971. (AD-741249, FAA-RD-72-31.)
3. Diehl, Larry A.: Measurement of Gaseous Emissions from an Afterburning Turbojet Engine at Simulated Altitude Conditions. NASA TM X-2726, 1973.
4. German, R. C.; High, M. D.; and Robinson, C. E.: Measurement of Exhaust Emissions from a J85-GE-5B Engine at Simulated High-Altitude Supersonic Free-Stream Flight Conditions. ARO-PWT-TR-73-49, ARO, Inc., 1973. (AD-764-717, AEDC-TR-73-103, FAA RD-73-92.)
5. Davidson, D. L.; and Domal, A. F.: Emission Measurements of a J93 Turbojet Engine. ARO-ETF-TR-73-46, ARO, Inc., 1973. (AD-766648, AEDC-TR-73-132.)
6. Holdeman, James D.: Exhaust Emission Calibration of Two J-58 Afterburning Turbojet Engines at Simulated High-Altitude, Supersonic Flight Conditions, NASA TN D-8173, 1976.
7. Pratt & Whitney JTF22 (F100). Jane's All the World's Aircraft 1979-80. Franklin Watts Inc., 1979, pp. 757-758.
8. Procedure for the Continuous Sampling and Measurement of Gaseous Emissions from Aircraft Turbine Engines. Aerospace Recommended Practice 1256, Oct. 1971, SAE.

TABLE III. - ENGINE INLET TEST CONDITIONS AND EXHAUST PROFILE DATA

FOR MACH 0.8 AT 9.14 KILOMETERS (30 000 ft)

(a) Intermediate (nonafterburning power; engine inlet temperature, 257 K; engine inlet pressure, 4.57 N/cm²; metered fuel-air ratio, 0.0124; exhaust nozzle radius, 31.75 cm

Radial distance from centerline, R/R _g	Exhaust-gas concentration				Gas sample fuel air ratio, faremiss	Exhaust total temperature		Exhaust total pressure, N/cm ²
	Carbon monoxide, ppmv	Carbon dioxide, ppmv	Hydrocarbons, ppmCv	Oxides of nitrogen, ppmv		K	R	
-0.998	317	13 091	0	51	0.006	546	982	11.75
-.798	218	21 081		91	.0095	680	1224	11.68
-.600	370	37 386		172	.0168	837	1507	11.87
-.398	405	41 735		197	.0187	901	1622	12.15
-.197	423	40 758		192	.0183	910	1638	12.95
0.	393	40 070		189	.0180	905	1630	10.45
.224	476	40 928		192	.0184	912	1641	13.04
.416	487	40 441		192	.0182	895	1611	12.38
.604	492	29 701		134	.0135	801	1442	11.85
.799	492	14 704		60	.0068	631	1136	11.55
1.014	461	4 364		15	.0021	476	856	10.69
Average	371	25 012		113	0.0113	696	1253	

(b) Maximum afterburning power; engine inlet temperature, 463 K; engine inlet pressure, 4.54 N/cm²; metered fuel-air ratio, 0.0603; exhaust nozzle radius, 45.95 cm

-1.002	1 070	32 061	753	5	0.0152	1156	2081	8.66
-.908	351	102 790	5	54	.0446	1925	3466	10.51
-.809	15 640	97 026	4234	1	.0513	1946	3504	10.33
-.708	15 070	99 179	4277	1	.0519	1886	3396	10.48
-.607	1 270	125 420	19	256	.0542	1900	3421	10.61
-.510	26	114 930	3	263	.0494	1836	3305	10.56
-.409	207	115 160	0	246	.0488	1824	3285	10.44
-.298	207	113 750		235	.0490	1804	3248	10.19
-.204	47	115 890		232	.0498	1810	3259	9.93
-.108	87	114 540		228	.0493	1793	3227	8.93
0.	63	112 850		224	.0486	1747	3145	8.97
.091	85	113 860		226	.0490	1755	3159	8.97
.191	74	112 990		226	.0487	1793	3228	8.94
.299	208	109 290		222	.0472	1749	3149	10.12
.390	210	108 670		222	.0470	1768	3182	10.37
.490	107	118 510		245	.0509	1884	3392	10.56
.591	3 838	126 380	7	244	.0557	1944	3500	10.75
.697	14 870	100 760	1941	2	.0512	1911	3440	10.78
.790	14 063	103 700	1272	1	.0516	1980	3564	10.70
.892	476	101 640	5	82	.0442	1951	3513	10.67
.990	1 765	37 622	4380	32	.0198	1234	2222	9.97
Average	4 781	101 948	962	115	0.0466	1809	3256	

TABLE IV. - ENGINE INLET TEST CONDITIONS AND EXHAUST PROFILE DATA
FOR MACH 0.8 AT 12.19 KILOMETERS (40 000 ft)

(a) Intermediate (noafterburning power; engine inlet temperature, 244 K; engine inlet pressure, 2.83 N/cm²; metered fuel-air ratio, 0.0125; exhaust nozzle radius, 31.85 cm

Radial distance from centerline, R/Rg	Exhaust-gas concentration				Gas sample fuel air ratio, faremiss	Exhaust total temperature		Exhaust total pressure, N/cm ²
	Carbon monoxide, ppmv	Carbon dioxide, ppmv	Hydrocarbons, ppmCv	Oxides of nitrogen, ppmv		K	R	
-1.008	207	10 609	0 ↓	30	0.0048	504	908	9.65
-.809	293	17 838		52	.0081	627	1129	8.34
-.61	356	32 124		102	.0145	775	1395	8.59
-.405	367	37 219		126	.0168	851	1531	8.68
-.197	360	38 103		130	.0171	860	1548	9.18
0.	385	36 962		123	.0166	854	1538	7.57
.197	356	37 280		125	.0168	859	1546	9.19
.389	401	37 242		120	.0168	846	1523	8.90
.591	356	27 949		90	.0127	671	1208	8.58
.790	378	13 479		39	.0062	535	964	8.38
.978	370	11 266	32	.0052	458	825	8.40	
Average	325	22 467	0	71	0.0102	633	1140	

(b) Partial afterburning power; engine inlet temperature, 244 K; engine inlet pressure, 2.80 N/m²; metered fuel-air ratio, 0.0337; exhaust nozzle radius, 40.45 cm

-0.999	733	24 771	1058	10	0.0120	895	1611	7.31
-.896	1 516	39 029	3209	14	.0197	1383	2490	7.61
-.789	1 497	77 012	2185	41	.0356	1745	3142	7.48
-.702	931	99 658	250	107	.0437	1780	3205	7.55
-.597	485	83 062	44	127	.0365	1565	2817	7.59
-.492	82	60 315	48	117	.0267	1270	2286	7.59
-.392	0	49 383	116	93	.0220	1106	1990	7.76
-.292	214	43 505	155	90	.0195	967	1740	7.67
-.198	250	41 526	139	86	.0187	917	1650	7.66
-.093	255	38 959	203	67	.0176	913	1643	7.55
0.	245	35 736	312	58	.0162	903	1625	6.99
.099	216	37 996	328	66	.0172	912	1642	7.47
.209	208	41 856	763	73	.0191	922	1659	7.69
.300	207	44 886	856	77	.0205	963	1734	7.70
.403	99	51 894	340	91	.0232	1096	1973	7.81
.509	310	66 337	395	113	.0295	1341	2414	7.65
.606	737	89 903	87	124	.0395	1623	2922	7.63
.701	903	108 070	11	114	.047	1827	3289	7.72
.806	1 823	71 646	12	19	.032	1687	3037	7.54
.900	1 731	36 594	584	8	.0174	1311	2359	7.57
1.005	660	21 634	4797	6	.0124	864	1555	7.61
Average	870	61 063	800	68	0.0276	1362	2451	

(c) Maximum afterburning power; engine inlet temperature, 244 K; engine inlet pressure, 2.81 N/cm²; metered fuel-air ratio, 0.0620; exhaust nozzle radius, 46.4 cm

-0.998	563	21 069	0	3	0.0097	1186	2135	7.02
-.902	889	98 476	5	37	.0463	1837	3307	7.69
-.797	14 660	86 616	3791	59	.0475	1833	3300	7.66
-.698	13 079	91 738	3389	89	.0478	1815	3267	7.72
-.599	910	110 020	0	140	.0425	1791	3224	7.81
-.499	162	97 908	4	134	.0456	1716	3089	7.83
-.394	252	105 160	2	140	.0464	1743	3137	7.75
-.302	513	107 030	0	127	.0463	1765	3178	7.62
-.202	605	106 630	↓	120	.0419	1771	3189	7.59
-.098	659	95 926		97	.0447	1745	3142	7.25
0.	678	102 600		104	.0447	1728	3110	7.26
.103	684	99 805		110	.0435	1741	3135	7.48
.205	525	101 740		112	.0442	1747	3145	7.68
.296	362	97 723		109	.0425	1693	3048	7.78
.399	184	96 279		112	.0418	1681	3027	7.88
.500	269	103 070		127	.0447	1758	3164	7.89
.600	1 750	117 010		151	.0510	1843	3317	7.89
.712	12 500	94 963	942	99	.0472	1834	3301	7.89
.801	9 662	105 720	272	82	.0500	1881	3386	7.78
.898	1 554	86 407	185	25	.0384	1763	3173	7.78
1.002	1 496	25 909	4699	6	.0147	1047	1885	7.48
Average	4 237	92 378	722	84	0.0428	1713	3082	

TABLE V. - ENGINE INLET TEST CONDITIONS AND EXHAUST PROFILE DATA
FOR MACH 1.4 AT 12.19 KILOMETERS (40 000 ft)

(a) Intermediate (nonafterburning power; engine inlet temperature, 303 K; engine inlet pressure, 5.95 N/cm²; metered fuel-air ratio, 0.0111; exhaust nozzle radius, 35.49 cm

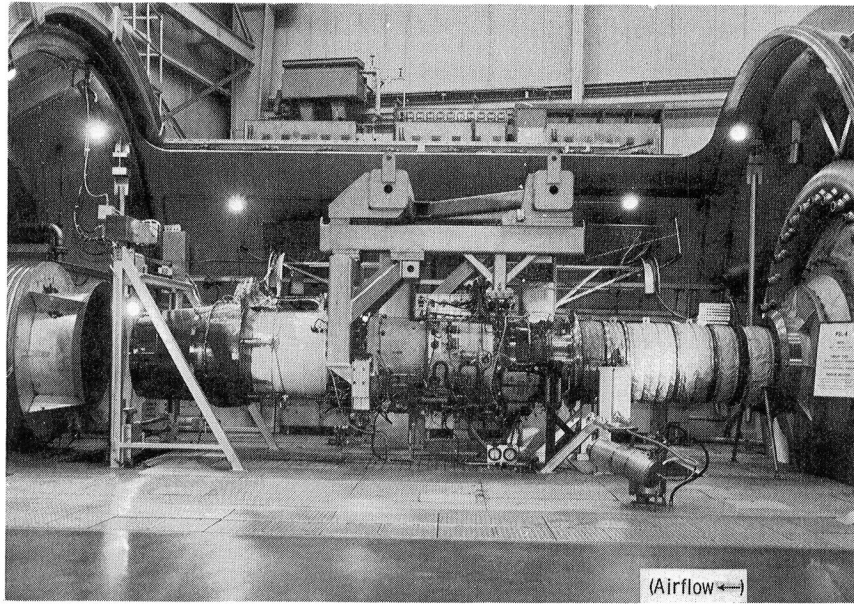
Radial distance from centerline, R/Rg	Exhaust-gas concentration				Gas sample fuel air ratio, faremiss	Exhaust total temperature		Exhaust total pressure, N/cm ²
	Carbon monoxide, ppmv	Carbon dioxide, ppmv	Hydrocarbons, ppmCv	Oxides of nitrogen, ppmv		K	R	
-0.594	6	40 600	0	204	0.0181	813	1464	11.63
-0.396	10	44 001		229	.0196	872	1569	11.65
-0.196	12	43 003		226	.0191	919	1655	11.65
0.	9	42 448		224	.0189	916	1649	8.57
.200	3	43 118		231	.0192	919	1655	11.69
.399	9	42 717		228	.0190	876	1576	11.49
.600	12	30 407		154	.0136	756	1361	11.65
.794	0	11 105		46	.0053	548	986	11.63
1.099	0	5 622		20	.0027	386	695	5.94
Average	3.0	20 257	0	103	0.0091	501	902	

(b) Partial afterburning power; engine inlet temperature, 301 K; engine inlet pressure, 5.94 N/cm²; metered fuel-air ratio, 0.0307; exhaust nozzle radius, 45.1 cm

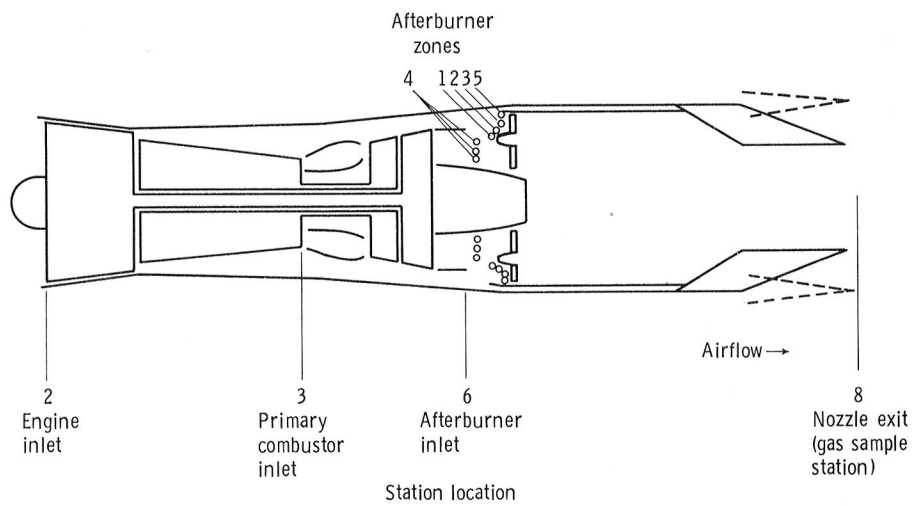
-0.998	2 304	18 687	4156	2	0.0115	853	1535	8.87
-.699	0	38 511	3587	3	.0219	1193	2147	9.43
-.799		85 279	132	21	.0384	1676	3017	9.46
-.701		113 580	8	166	.0496	1832	3298	9.83
-.598		86 505	8	182	.0382	1624	2923	9.87
-.498	491	64 361	20	183	.0286	1364	2455	10.00
-.400	234	53 042	23	190	.0236	938	1689	10.02
-.298	125	46 378	18	200	.0207	996	1793	9.88
-.199	102	43 562	16	202	.0194	928	1671	8.44
-.089	122	42 546	24	190	.0190	887	1597	8.37
0.	150	42 635	40	178	.0190	885	1594	8.37
.099	227	43 249	68	163	.0194	900	1621	8.39
.203	447	45 021	149	134	.0203	944	1700	8.69
.297	0	48 518	248	107	.0220	1002	1805	9.79
.400		55 005	263	128	.0250	1410	2538	9.99
.500		71 062	52	157	.0318	1434	2582	10.07
.608		96 960	6	166	.0427	1742	3137	10.07
.700		105 970	7	95	.0464	1868	3362	10.05
.800		54 901	1654	5	.0275	1468	2642	9.87
1.002	0	9 587	3607	2	.0130	561	1010	8.82
Average	52.61	61 847	1001	93.5	0.0295	1296	2332	

(c) Maximum afterburning power; engine inlet temperature, 301 K; engine inlet pressure, 5.95 N/cm²; metered fuel-air ratio, 0.0549; exhaust nozzle radius, 51.2 cm

-1.00	1 163	28 470	1690	22	0.0141	1086	1955	9.38
-.904	494	85 316	8	68	.0374	1787	3217	9.94
-.805	8 268	121 890	40	124	.0558	2013	3623	10.37
-.707	11 615	115 230	145	4	.0547	1983	3570	10.66
-.601	641	128 520	0	366	.0552	1963	3533	10.74
-.501	81	117 200		357	.0504	1868	3363	10.67
-.409	11	112 320		336	.0484	1816	3270	10.50
-.307	3	109 670		320	.0473	1788	3218	10.19
-.205	44	109 320		311	.0471	1759	3166	9.34
-.106	12	107 710		305	.0465	1767	3181	9.44
0.	4	106 830		302	.0461	1716	3089	9.50
.093	30	108 880		305	.0470	1708	3075	9.51
.192	24	108 350		309	.0467	1708	3074	9.39
.293	207	106 440		307	.0460	1726	3107	10.05
.394	7	110 620		321	.0477	1799	3239	10.29
.497	229	122 170		352	.0524	1921	3459	10.51
.597	2 175	130 720		350	.0567	1970	3547	10.57
.696	11 131	116 370	104	8	.0548	1954	3518	10.62
.801	623	117 780	0	130	.0508	1946	3503	10.30
.891	2 040	60 814	1218	50	.0284	1541	2774	9.88
.999	874	18 896	4458	17	.0111	803	1445	9.32
Average	3 086	100 832	273	165	0.0445	1754	3157	

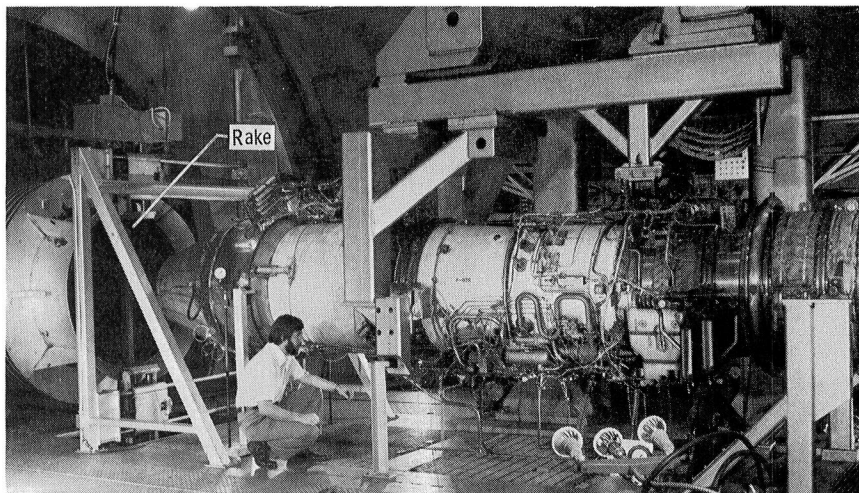


(a) Installed in altitude test chamber.

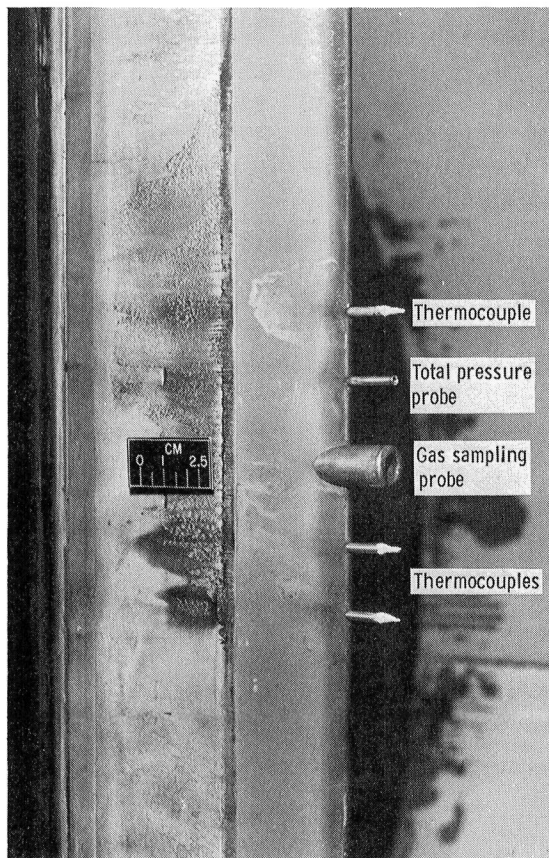


(b) Engine instrumentation locations.

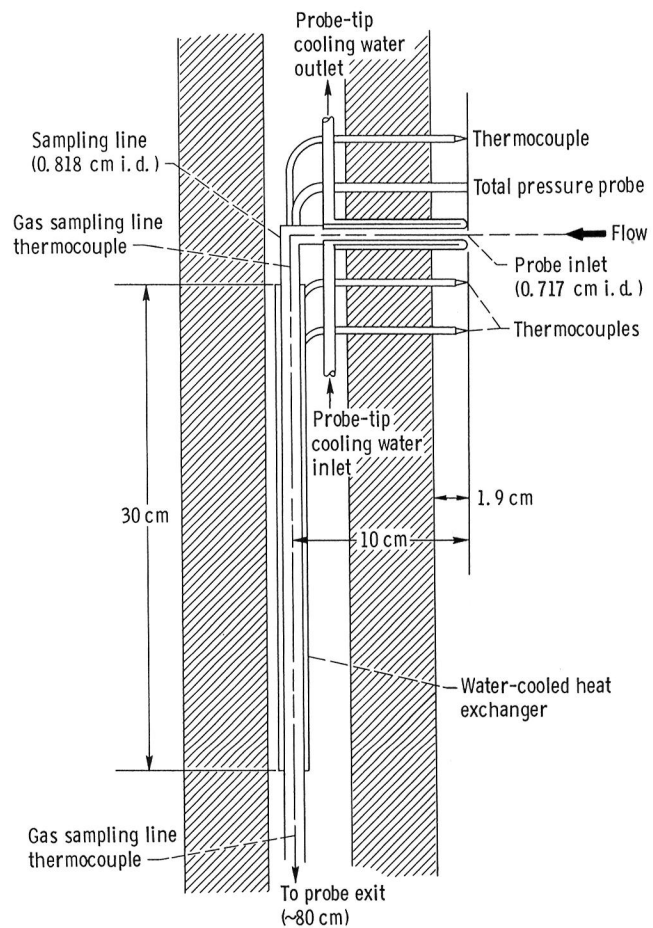
Figure 1. - Afterburning turbofan engine.



(a) Installation.

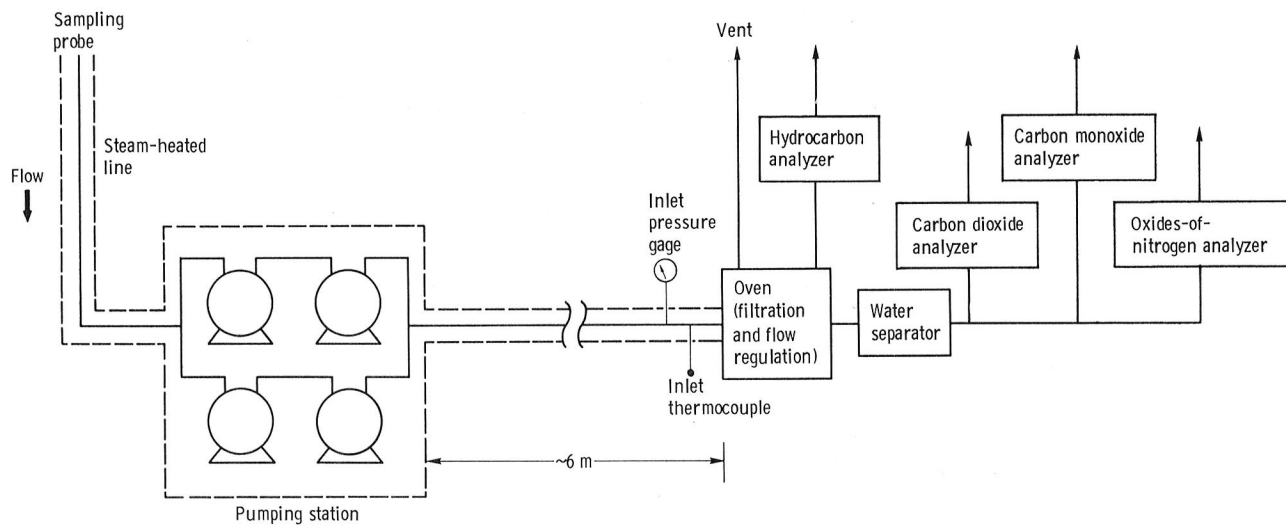


(b) Detail of sensor area.

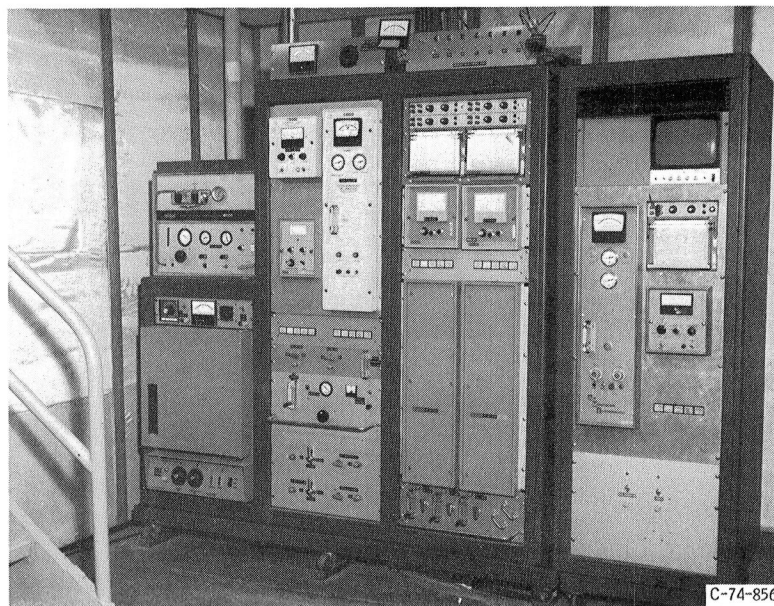


(c) Schematic of gas sample probe.

Figure 2. - Probe and traversing mechanism.



(a) Flow schematic.



(b) Test cell setup.

Figure 3. - Console-gas analysis system.

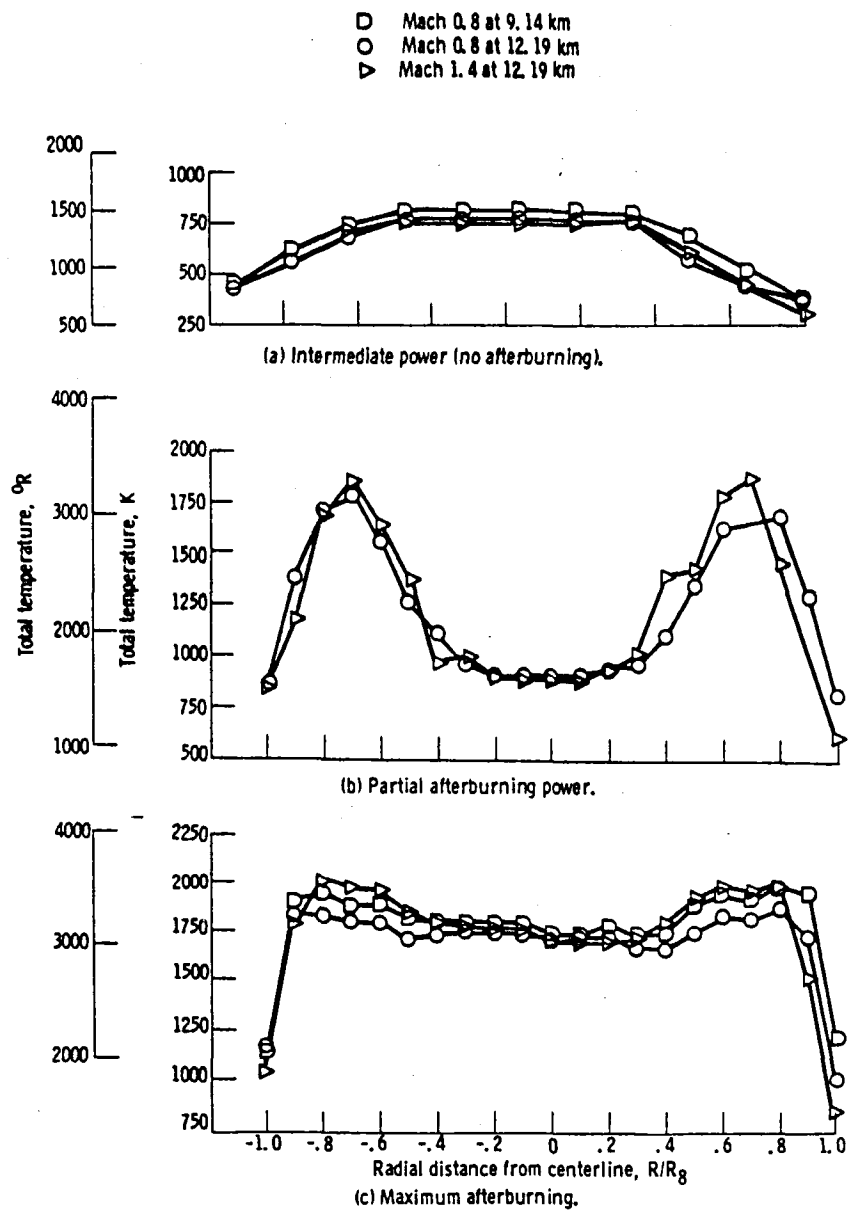


Figure 4. - Total temperature distribution.

- Mach 0.8 at 9.14 km
- Mach 0.8 at 12.19 km
- ▽ Mach 1.4 at 12.19 km

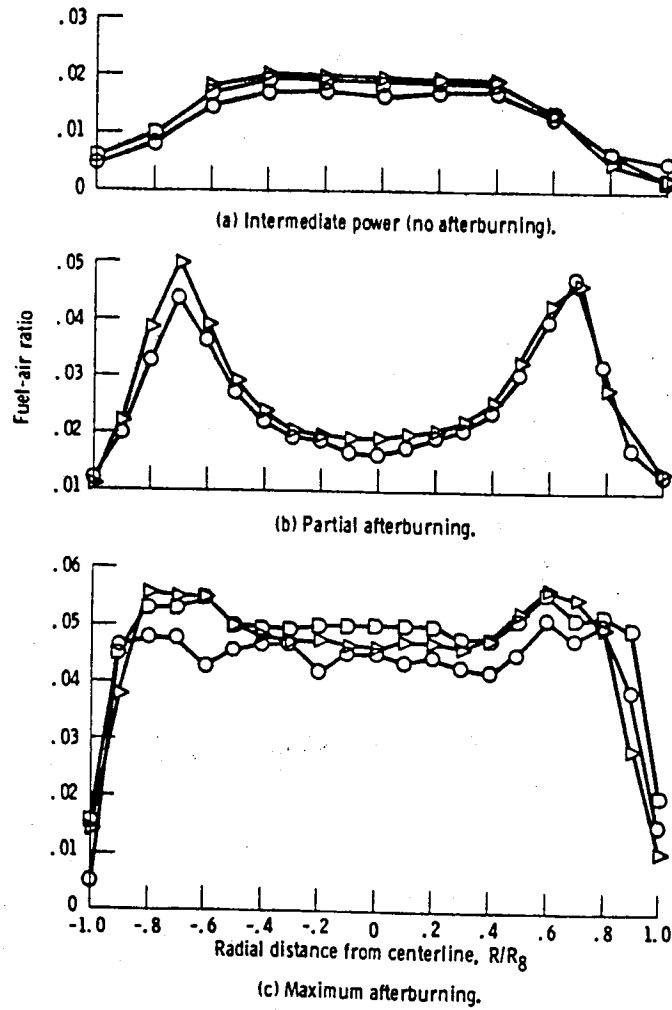


Figure 5. - Local fuel-air ratio profile.

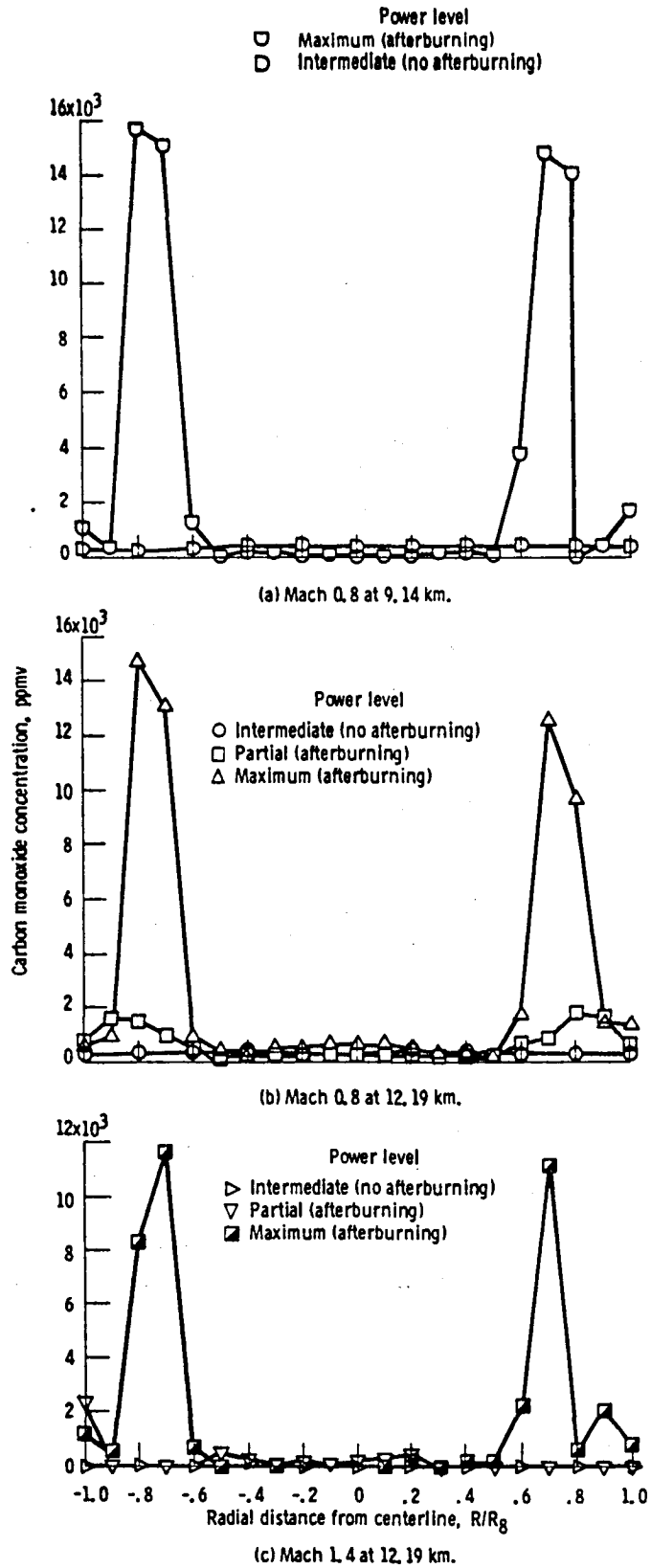


Figure 6. - Carbon monoxide concentration profiles.

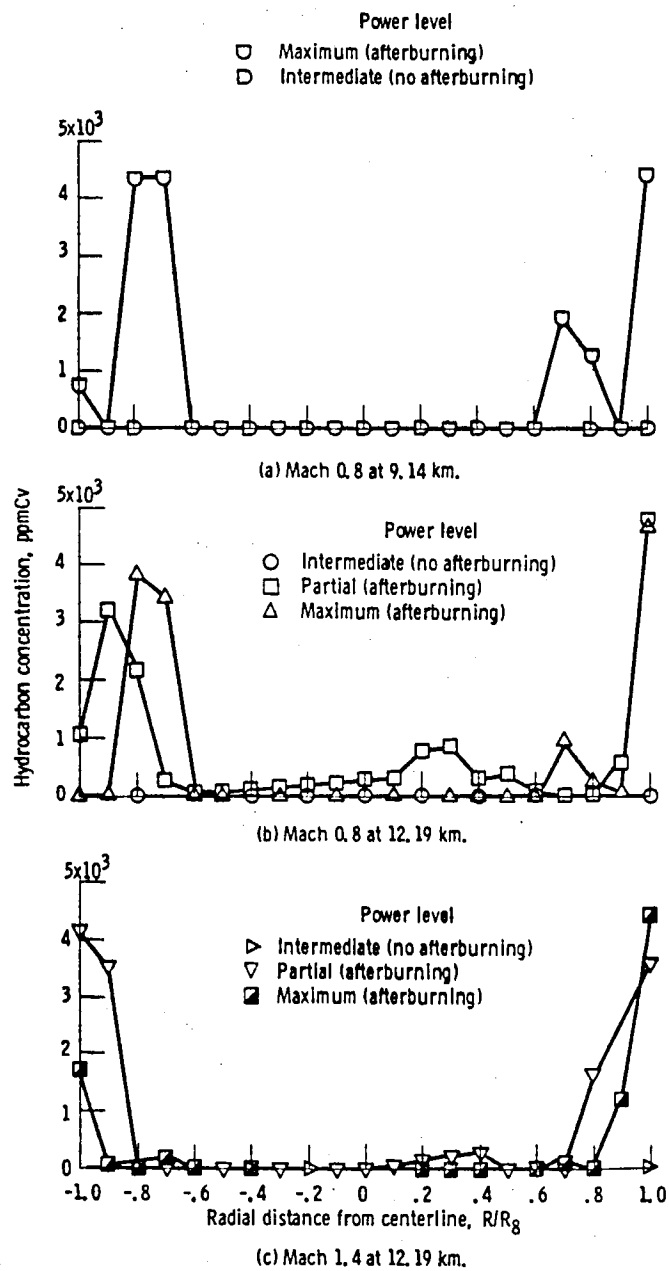


Figure 7. - Hydrocarbon concentration profiles.

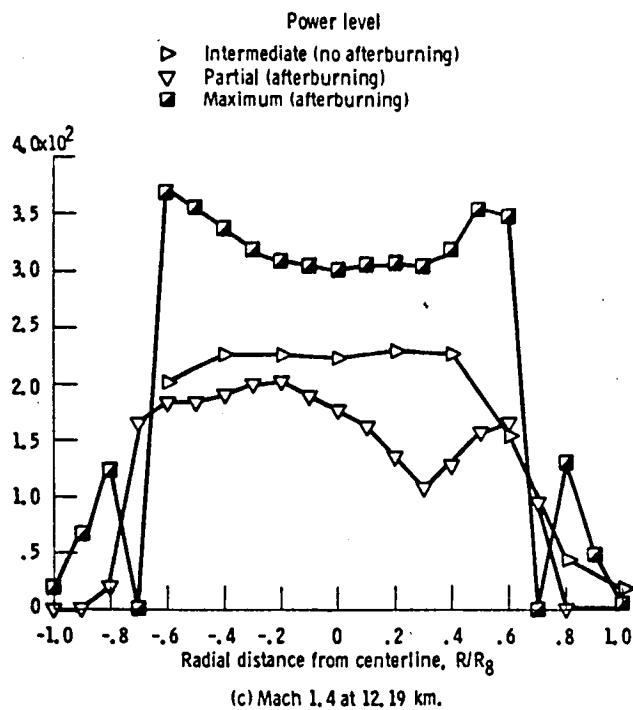
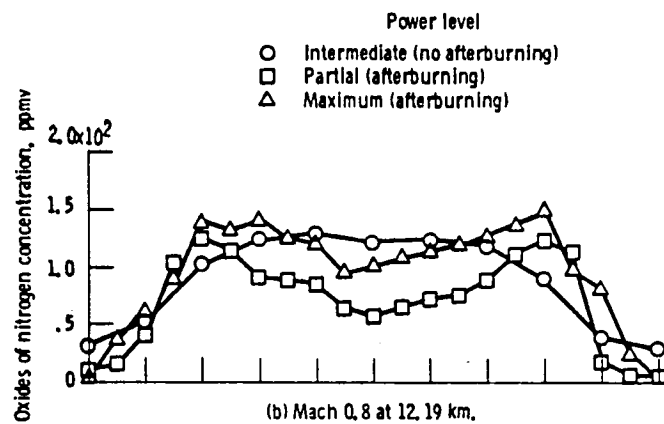
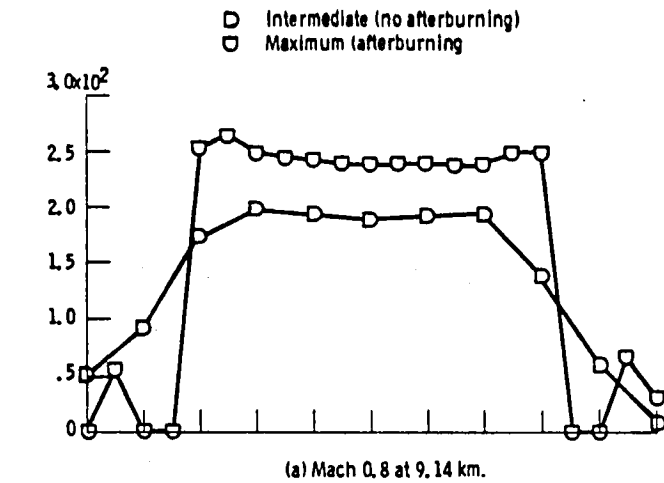


Figure 8. - Oxides of nitrogen concentration profiles.

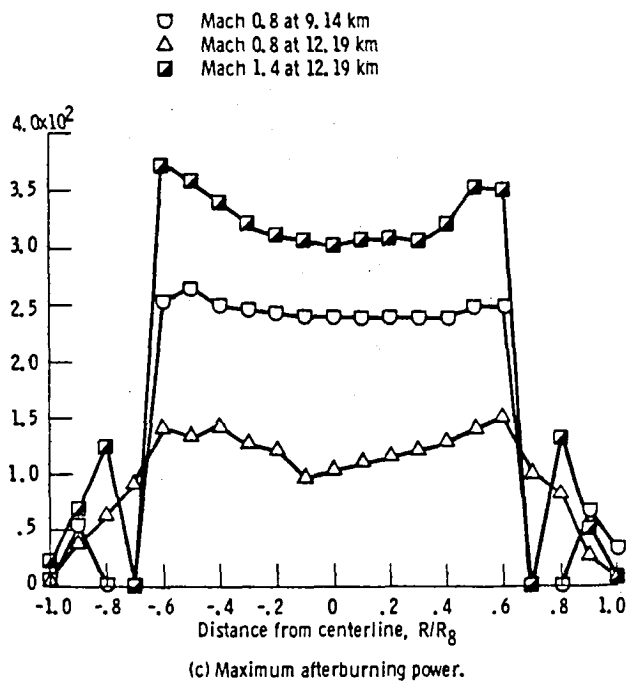
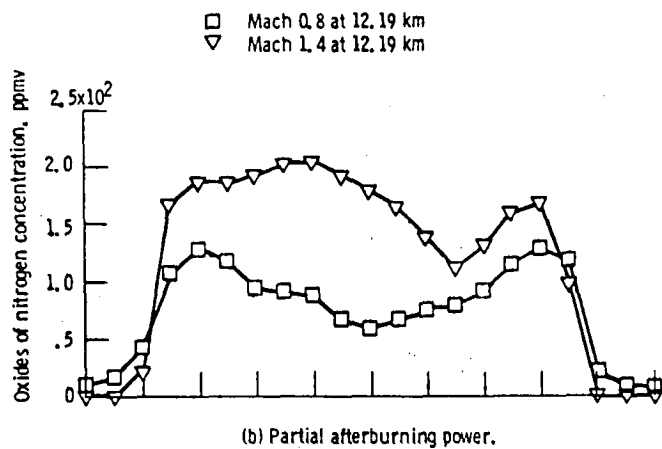
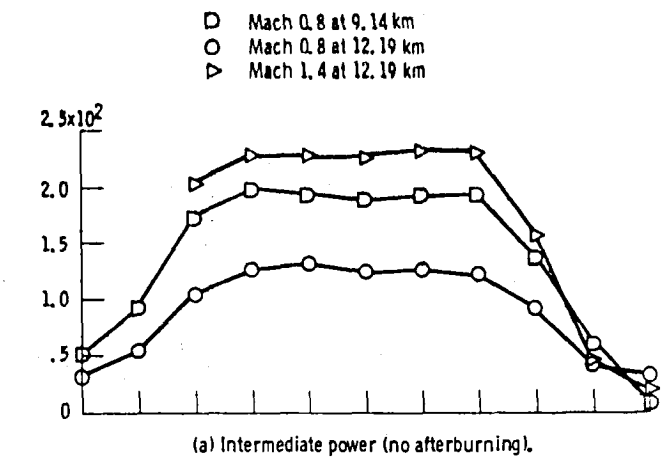
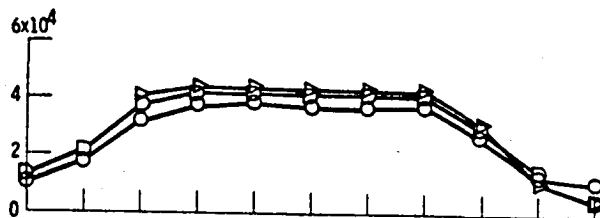
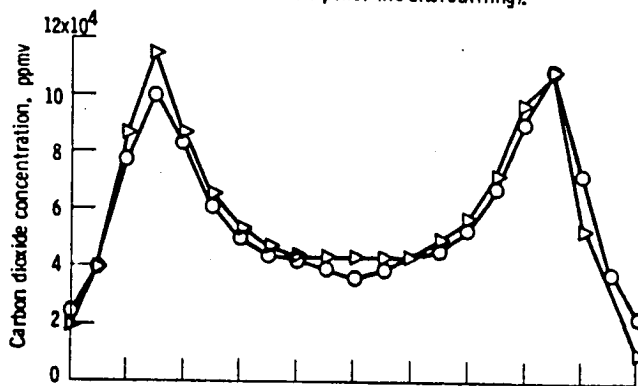


Figure 9. - Oxides of nitrogen concentration profiles.

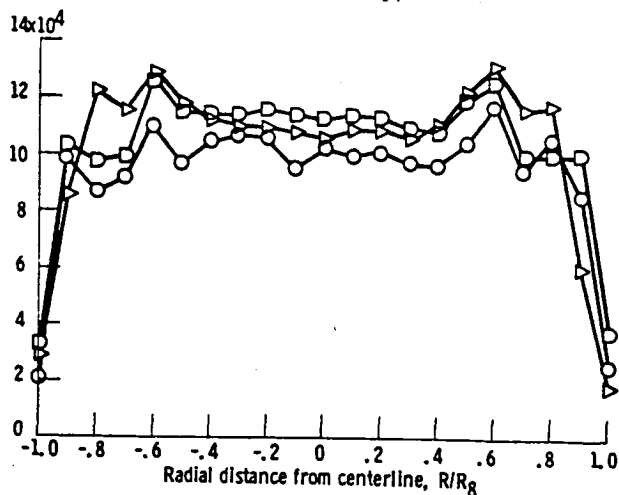
- Mach 0.8 at 9.14 km
- Mach 0.8 at 12.19 km
- △ Mach 1.4 at 12.19 km



(a) Intermediate power (no afterburning).



(b) Partial afterburning power.



(c) Maximum afterburning power.

Figure 10. - Carbon dioxide concentration profiles.

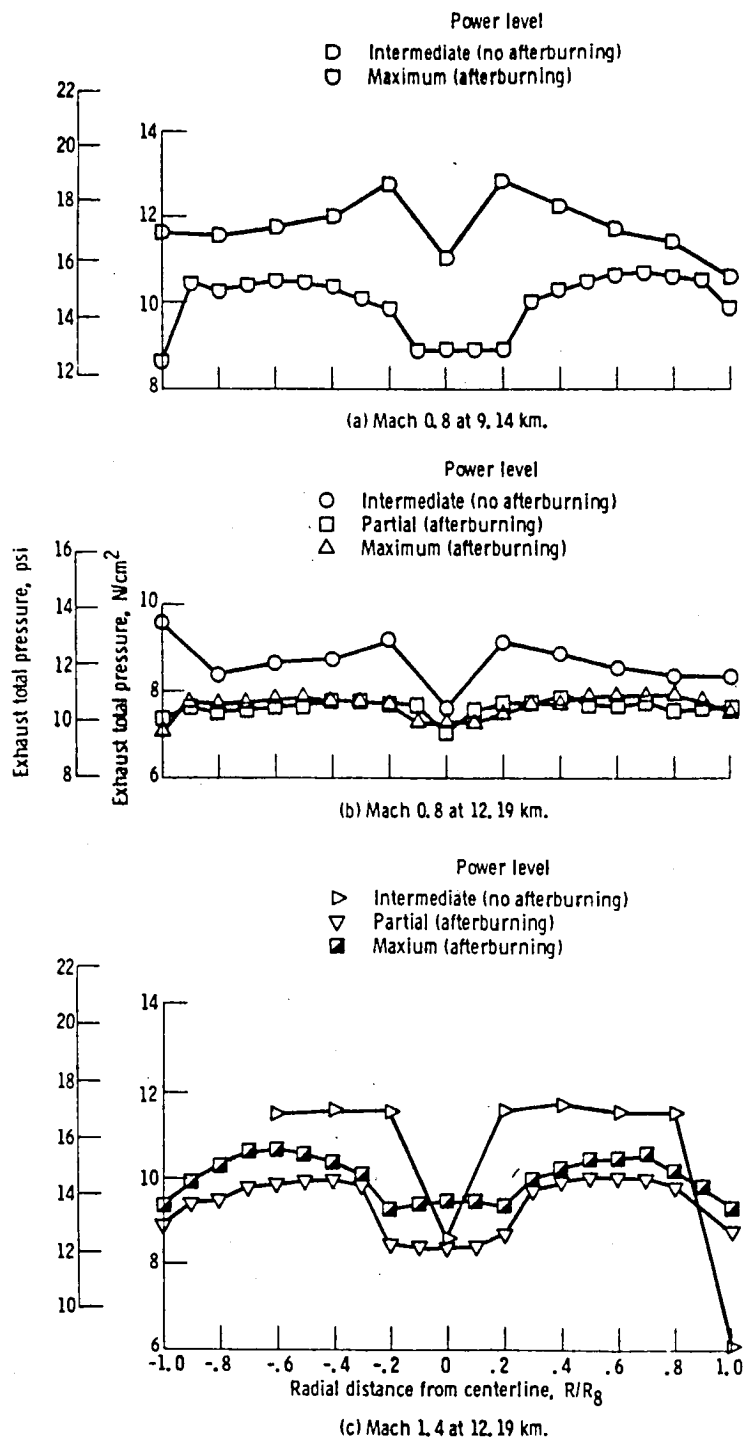


Figure 11. - Exhaust total-pressure concentration profiles.

	Power level	Mach number	Altitude, km
○	Intermediate	0.8	9.14
◻	Maximum afterburning	0.8	9.14
○	Intermediate	0.8	12.19
◻	Partial afterburning	0.8	12.19
△	Maximum afterburning	0.8	12.19
▽	Intermediate	1.4	12.19
▽	Partial afterburning	1.4	12.19
◻	Maximum afterburning	1.4	12.19

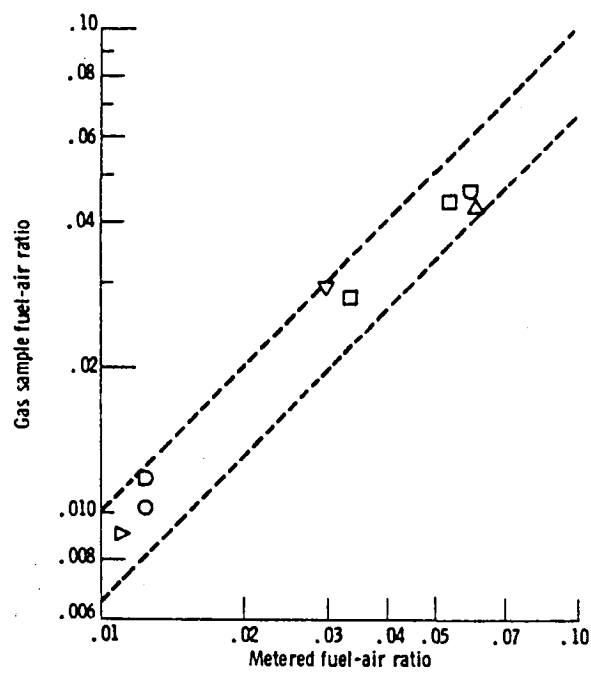


Figure 12. - Comparison of gas sample and metered fuel-air ratio.

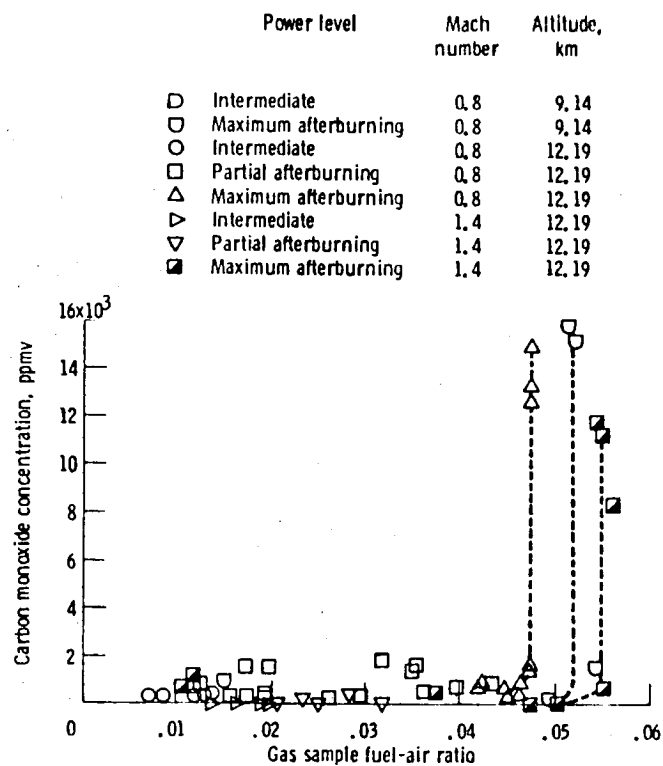


Figure 13. - Variation of carbon monoxide with gas sample fuel-air ratio.

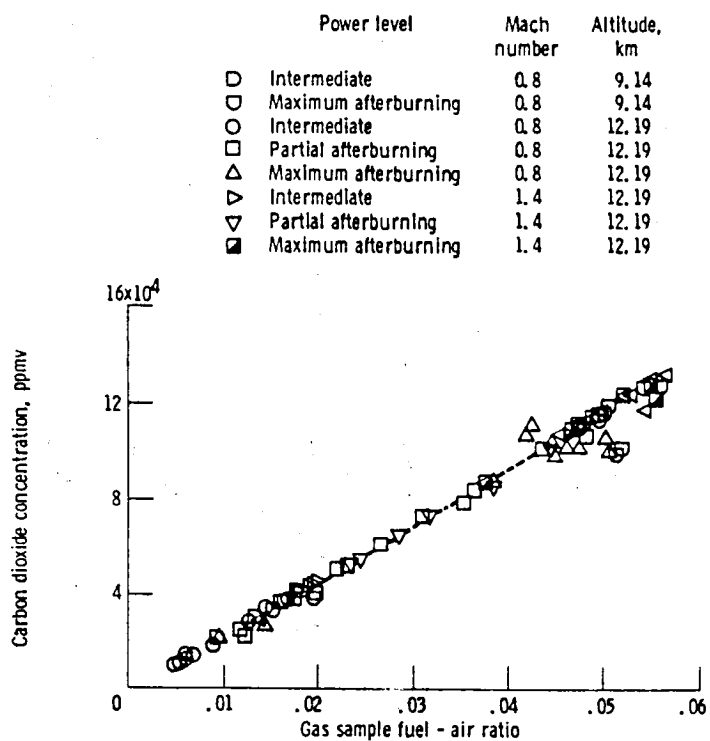


Figure 14. - Variation of carbon dioxide with gas sample fuel-air ratio.

	Power level	Mach number	Altitude, km
□	Intermediate	0.8	9, 14
○	Maximum afterburning	0.8	9, 14
○	Intermediate	0.8	12, 19
□	Partial afterburning	0.8	12, 19
△	Maximum afterburning	0.8	12, 19
▽	Intermediate	1, 4	12, 19
▽	Partial afterburning	1, 4	12, 19
■	Maximum afterburning	1, 4	12, 19

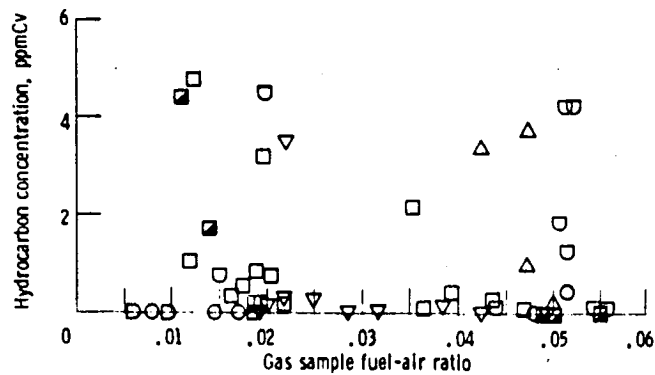


Figure 15. - Variation of hydrocarbon with gas sample fuel-air ratio.

	Power level	Mach number	Altitude, km
□	Intermediate	0.8	9, 14
○	Maximum afterburning	0.8	9, 14
○	Intermediate	0.8	12, 19
□	Partial afterburning	0.8	12, 19
△	Maximum afterburning	0.8	12, 19
▽	Intermediate	1, 4	12, 19
▽	Partial afterburning	1, 4	12, 19
■	Maximum afterburning	1, 4	12, 19

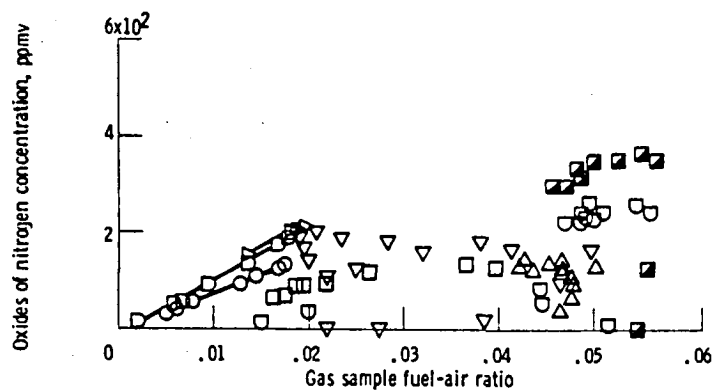


Figure 16. - Variation of oxides of nitrogen with gas sample fuel-air ratio.

1. Report No. NASA TM-81656		2. Government Accession No.		3. Recipient's Catalog No.	
4. Title and Subtitle EXHAUST EMISSION SURVEY OF AN F100 AFTERBURNING TURBOFAN ENGINE AT SIMULATED ALTITUDE FLIGHT CONDITIONS				5. Report Date March 1981	
				6. Performing Organization Code 505-32-62	
7. Author(s) John E. Moss, Jr. and Richard R. Cullom				8. Performing Organization Report No. E-673	
9. Performing Organization Name and Address National Aeronautics and Space Administration Lewis Research Center Cleveland, Ohio 44135				10. Work Unit No.	
				11. Contract or Grant No.	
12. Sponsoring Agency Name and Address National Aeronautics and Space Administration Washington, D.C. 20546				13. Type of Report and Period Covered Technical Memorandum	
				14. Sponsoring Agency Code	
15. Supplementary Notes					
16. Abstract Emissions of carbon monoxide, total oxides of nitrogen, unburned hydrocarbons, and carbon dioxide from an F100, afterburning, two-spool turbofan engine at simulated flight conditions are reported herein. Test conditions included simulated flight at Mach 0.8 for altitudes of 9.14 and 12.19 km and Mach 1.4 at 12.19 km. For each flight condition emission measurements were made for two or three power levels from intermediate power (nonafterburning) through maximum afterburning. The data showed that emissions vary with flight speed, altitude, power level, and radial position across the nozzle. Carbon monoxide emissions were low for intermediate power (nonafterburning) and partial afterburning, but regions of high CO were present downstream of the flame holder at maximum afterburning. Unburned hydrocarbon emissions were low for most of the simulated flight conditions. The local NO _x concentrations and their variability with power level increased with increasing flight Mach number at constant altitude, and decreased with increasing altitude at constant Mach number. Carbon dioxide emissions were proportional to local fuel-air ratio for all conditions.					
17. Key Words (Suggested by Author(s)) Exhaust gases; Afterburning, F100 engines; Turbofan engine; Air pollution; Combustion products				18. Distribution Statement Unclassified - unlimited STAR Category 07	
19. Security Classif. (of this report) Unclassified		20. Security Classif. (of this page) Unclassified		21. No. of Pages	
				22. Price*	

National Aeronautics and
Space Administration

Washington, D.C.
20546

Official Business
Penalty for Private Use, \$300

SPECIAL FOURTH CLASS MAIL
BOOK

Postage and Fees Paid
National Aeronautics and
Space Administration
NASA-451



NASA

POSTMASTER: If Undeliverable (Section 158
Postal Manual) Do Not Return
